Quantitative measurement and real-time tracking of high intensity focused ultrasound using phase-sensitive optical coherence tomography

Le, Nhan; Song, ShaoZhen; Nabi, Ghulam; Wang, Ruikang; Huang, Zhihong

Published in:
International Journal of Hyperthermia

DOI:
10.1080/02656736.2016.1190036

Publication date:
2016

Document Version
Peer reviewed version

Quantitative measurement and Real-time tracking of High Intensity Focused Ultrasound using Phase-Sensitive Optical Coherence Tomography: Feasibility study

Nhan Le[1]; ShaoZhen Song[2]; Ghulam Nabi[3]; Ruikang Wang[2]; Zhihong Huang[1]

University of Dundee, Dundee, UK

University of Washington, USA

Ninewells Hospital, Dundee, UK

Abbreviation

HIFU High-Intensity Focused Ultrasound, general term, including but not limited to Focused Ultrasound Surgery

FUS Focused Ultrasound Surgery, a medical term for procedure of using HIFU to ablate a particular region of tissue

SW-OCE Shear-wave Optical Coherence Elastography

PhS-OCT Phase-Sensitive Optical Coherence Tomography

This is an Accepted Manuscript of an article published by Taylor & Francis in *International Journal of Hyperthermia* on 5 July 2016, available online:
http://www.tandfonline.com/10.1080/02656736.2016.1190036

ABSTRACT

Phase-Sensitive Optical Coherence Tomography (PhS-OCT) is proposed, as a new High-Intensity Focused Ultrasound (HIFU) imaging guidance, to detect and track HIFU focus inside 1% Agar sample in this work. The experiments studied the effect of varying HIFU power on the induction of shear-wave, which can be implemented as a new technique to monitor Focused Ultrasound Surgery (FUS).

Miniature HIFU transducer (1.02 MHz, 20 mm diameter, 11 mm focal length) was produced in-house, pressure-field mapped, and calibrated. The transducer was then embedded inside 1%-agar phantom, which is placed under PhS-OCT for observation, under various HIFU power settings (acoustic power, and number of cycles per pulse).

Shear-wave was induced on the sample surface by HIFU, and was captured in full under PhS-OCT. The lowest HIFU acoustic power output for the detection of shear-wave was found to be 0.36 W (1.02 MHz, 100 cycles/pulse), or with the number of cycles/pulse as low as 20 (1.02 MHz, 0.98W acoustic power output).

A linear relationship between acoustic power output and the maximum shear-wave displacement was found in the first study. The second study explores a non-linear correlation between the (HIFU) numbers of cycles per pulse, and the maximum shear-wave displacement.

PhS-OCT demonstrates excellent tracking and detection of HIFU-induced shear-wave. The results could benefit other imaging techniques in tracking, and guiding HIFU focus. Further studies will explore the relationship between the physical transducer characteristics and the HIFU-induced shear-wave.

INTRODUCTION

High-Intensity Focused Ultrasound (HIFU) is a general term for the application of high-power ultrasonic wave within a well-defined focus. One clinical application of HIFU is known as Focused Ultrasound Surgery, where HIFU is mainly used as a hyperthermia therapy.

As HIFU delivers high-energy and pro-longed ultrasonic pulse into biological tissue within a well-defined focus, the temperature at said focus elevates quickly above hyperthermia threshold in a few seconds(1). Relying on hyperthermia effect of HIFU, Magnetic Resonance Imaging and Ultrasound Imaging has been adapted in the past for planning and guiding FUS. Imaging guidance in FUS is extremely important as any form of unwanted and/or extensive tissue damage can be minimised.

Each Imaging guidance modality has different approach in imaging, tracking and guiding FUS. In particular, MRI imaging measures the proton resonance frequency shift, and produces a real-time temperature map of tissue (within a region of interest). This imaging technique was introduced in the late 1980s (2), and is known as MR Thermometry nowadays. It takes MR Thermometry another decade until this imaging technique was first introduced for monitoring HIFU and subsequently in FUS (3, 4). MR Thermometry has been developed and improved ever since to enhance its capabilities in real-time thermometry, e.g. reducing susceptibility in patient breathing motion, inhomogeneity within the tissues, etc. Despite many great progresses, MR Thermometry technique is still relatively expensive to maintain and operate. The imaging technique also requires certain level of temperature elevation (above hyperthermia threshold) in the targeted tissue in order to track the HIFU focus.

Ultrasound imaging (sonography in medical term), on the other hand, is relatively inexpensive and has been employed in almost every clinical settings. The main ultrasound-imaging techniques for guiding FUS include B-mode sonography (5), and elastography (6). There are limitations in each ultrasound imaging technique, namely 1) lack of contrast between the echoic signals of the surrounding tissue and the HIFU lesions in B-mode imaging, and 2) limited real-time monitoring in Elastography as the ablated region only becomes visible after damage to tissue has occurred. In normal B-mode imaging,

the formation of bubble (or cavitation) clouds often indicates the activity at HIFU-focus. However, this technique requires HIFU to operate at high-power settings and is likely to cause mechanical damage to tissues. On the other hand, sono-elastography differentiates the elasticity difference between the HIFU-induced lesion and the surrounding tissue. However, the elasticity changes in tissue only occur when tissue undergoes drastic and irreversible denaturation process (caused by hyperthermia).

Phase-sensitive Optical Coherence Tomography (PhS-OCT) is introduced in this work as a new imaging technique to monitor and calibrate HIFU procedure in real-time, at sub-therapeutic HIFU power level. The approach of this new HIFU imaging guidance is fundamentally different from the rest, where it captures HIFU-induced shear-wave, and uses the acquired information to locate the HIFU focusing. This imaging technique also benefits from very high resolution and sensitivity over small deformation(7). In particular, PhS-OCT is capable of capturing shear-wave with the imaging rate of up to 46.8 kHz and axial resolution of less than 1 nm in our system. Therefore, PhS-OCT was adapted in this work for tracking HIFU in real-time, and calibrating the HIFU power appropriately for tracking and monitoring purposes. Shear-wave induced by HIFU is studied at different HIFU power settings and different pulse length. The result of this study will demonstrate and provide a new method for tracking, and monitoring HIFU procedure, especially complimenting the newly adopted shear-wave ultrasound Imaging (8).

MATERIALS AND METHODS

1. High-Intensity Focused Ultrasound (HIFU) transducer

High-Intensity Focused Ultrasound (HIFU) transducer was fabricated in-house from PZ-54 material focusing bowl (Meggitt Sensing Systems, Denmark). The focusing bowl has resonant frequency at 1.02 MHz, 20 mm in diameter, and 11 mm focal length. The backing material is composite epoxy (epoFix and glass microsphere, weight ratio 60:40 respectively). The quarter-wave impedance matching layer is made of silver-epoxy.

The acoustic power output of the HIFU transducer (1.02 MHz, 20 mm diameter, 11 mm focal length) was calibrated using radiation force balance (Precision Acoustic Ltd.). The pressure field around HIFU focus is mapped using 0.5 mm needle hydrophone (Precision Acoustic Ltd.) mounted on 3D-Stepping motor (Velmex, USA) with linear stepping motor, resolution of 0.02 mm.

a. Pressure field mapping

The acoustic pressure was recorded at each location around the HIFU focus, forming a 2D pressure field map. The relative intensity acoustic map (Figure 1a) was tabulated from a 2D pressure field map (20 mm range in axial direction, 8 mm range in lateral direction, 0.02 mm resolution in both directions), by:

$$I_r(i,j) = \frac{I_{ij}}{I_{max}} = \frac{p_{ij}^2}{p_{max}^2}$$

where i and j being pixel coordinates of column and row, p_{max} is the maximum pressure found in the 2D pressure map.

The logarithm of the intensity mapping (Figure 1b) was converted from the pressure field mapping using the equation:

$$L_I(i,j) = 10log_{10}(I_r(i,j)) = 20log_{10}\left(\frac{p_{ij}}{p_{max}}\right)$$

where $L_I(i,j)$ is the relative intensity in logarithmic scale at (i,j) coordinates.

The relative HIFU intensity map and its logarithmic scale help approximating PhS-OCT scanning range for spatial and temporal resolution optimization. Since the full width at half-maximum (FWHM) intensity is less than 2.0 mm in lateral dirrection, the PhS-OCT scanning range was set at 2.5 mm.

Note that the fringes at the HIFU-focus is due to focus positioning in the near-field diffraction region.

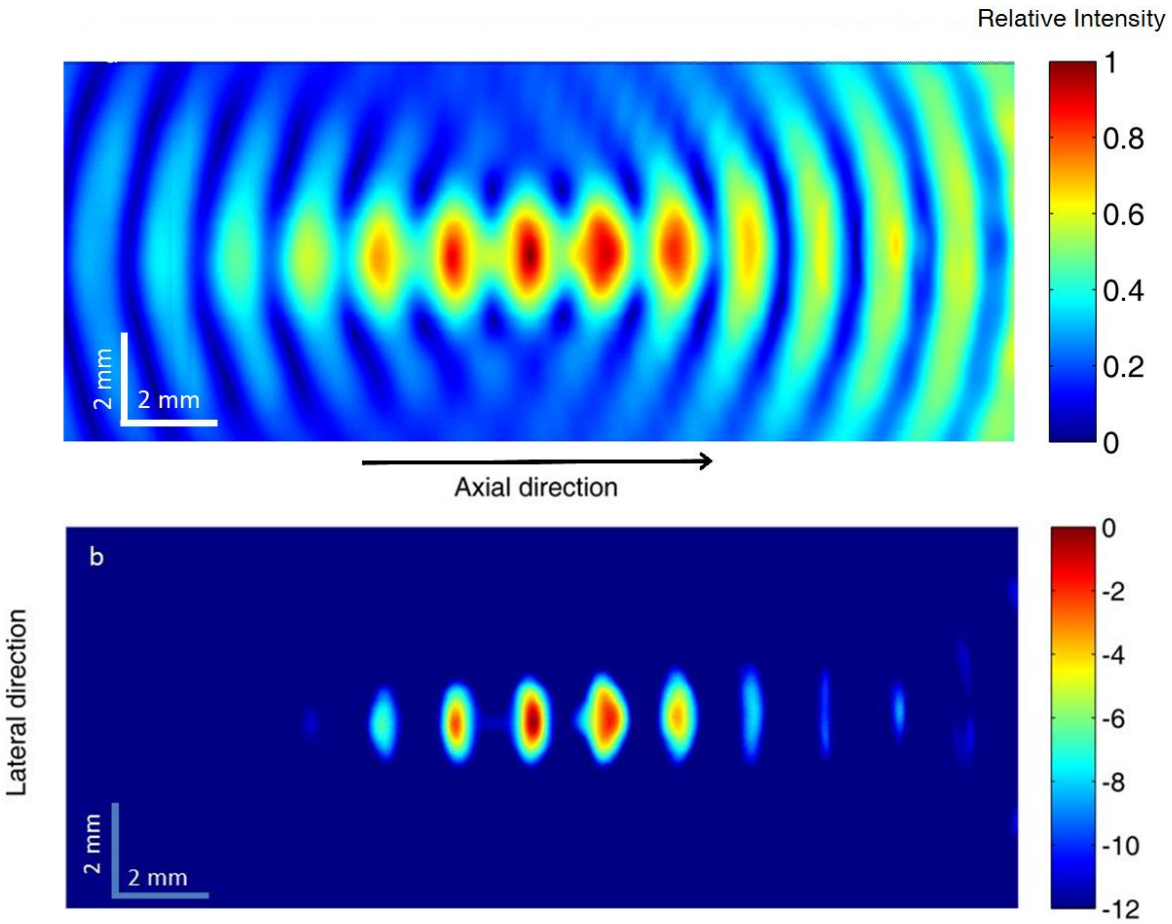

Figure 1: a) Relative intensity map and b) logarithm intensity map of the HIFU transducer in the axial plane of the focus

b. Acoustic power output

HIFU acoustic power output is an important parameter for quantifying the intensity of an acoustic pulse. The acoustic power output needs to be predictable with a reference input power (or any other similar parameter) that can be read easily. Since pre-amplified voltage from signal generator provides simple reference to the acoustic power output, HIFU transducer was calibrated against the pre-amplified voltage readings. This direct reference is convenient for performing experiments, since the RF power output (from RF Power amplifier) vs Acoustic power output (from HIFU transducer) is non-linear due to imperfections in the power amplify and power transfer/impedance matching circuit at high-frequency. Harmonic frequency is usually present in the amplified voltage waveform.

A typical result between the output signal from signal generator (V) and the HIFU acoustic power output (W) is shown in Figure 2. This acoustic power output will be the prime parameter for quantifying the power of a HIFU pulse in this paper.

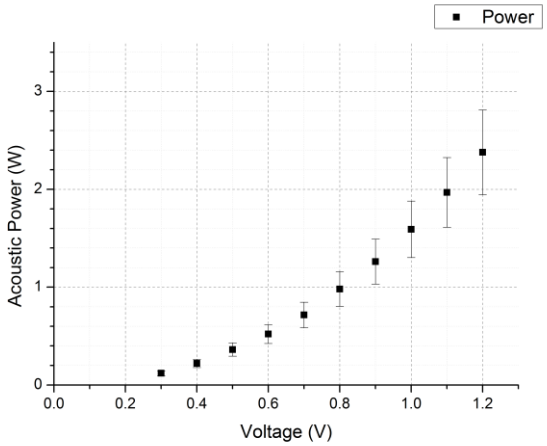

Figure 2 Signal generator's input signal vs. HIFU acoustic power output

2. Phase-Sensitive Optical Coherence Tomography (PhS-OCT)

Phase-Sensitive Optical Coherence Tomography was developed by Bioinstrumentation and Optics group at University of Dundee, based on phase detection between each consecutive frames (7). The PhS-OCT uses broadband laser source and is a spectral-domain optical coherence tomography setup. The scanning mirror is a mirror galvanometer that is integrated into the PhS-OCT system for 2D scanning protocols.

The PhS-OCT (camera exposure 17.4 µs, sensitivity 450 e^-/count) performs a 46.8 kHz sampling rate (approximately 21.4 µs per frame), acquiring 256 frames over approximately 5.47 milliseconds (256 A-scan forming 1 M-scan), in each scan-line (forming 1 M-scan). The scan-line repeats across the imaging plane forming 256 M-scans. This results in a complete M-B-scan. The data format is 1024 pixel-depth x 256 frames x 256 scan-lines. The complete data acquisition takes approximately 2 seconds. Each B-scan (frame) was processed with respect to the previous one to determine the phase shift and thus, the displacement due to HIFU-induced shear-wave.

Figure 3 illustrates our scanning protocol in our experimental setup. The HIFU-pulse is constant amplitude for any given pulse length. The durations between pulses are only relative and not drawn to scale in Figure 3, unless expressly stated.

We have also developed real-time scanning software that utilizes the PhS-OCT to detect shear-wave propagation on-demand. Real-time PhS-OCT technique will be described in more details in a separate paper since it has a different approach and produces data at much lower spatial resolution. In summary, the software detects phase changes in signals between each consecutive scan-line, and not between each frame (assuming that the lateral resolution is small enough). This technique would minimise the total time required to accurately locate the shear-wave source, however, at the expense of reduced image quality. Final confirmation step is required to determine the exact location of HIFU focus within the agar sample, and will be described more in the result.

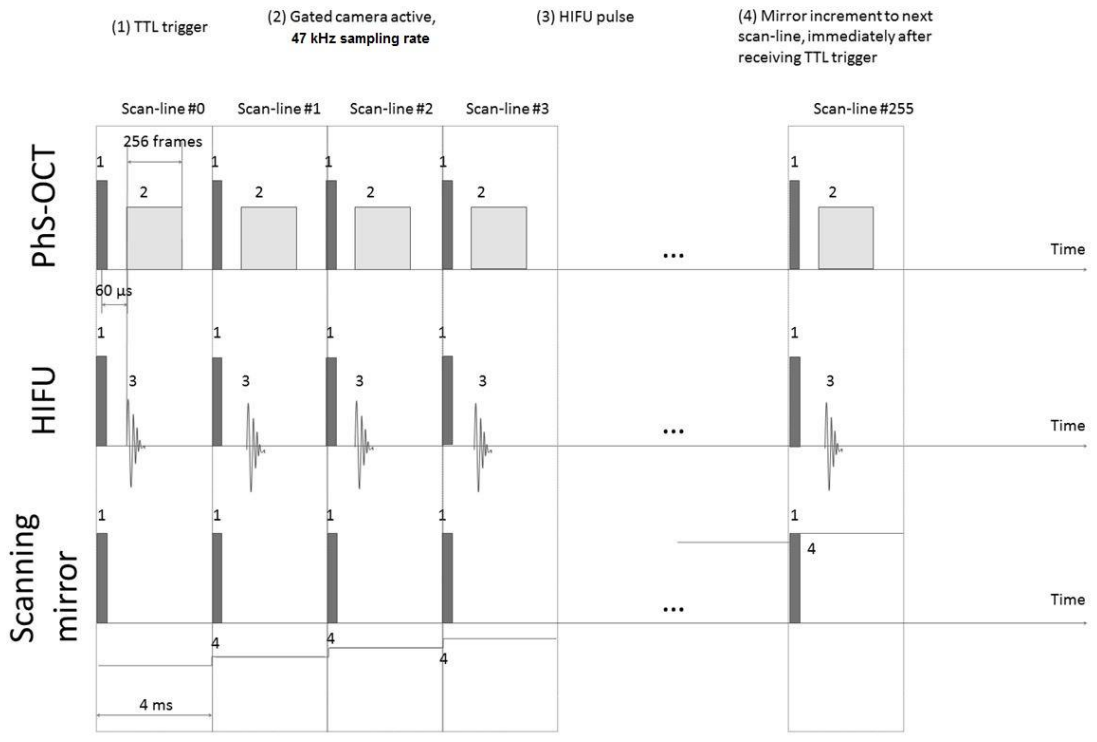

Figure 3: Scanning protocols for PhS-OCT and HIFU transducer for 2D capture of HIFU-induced shear-wave. (TTL trigger is sent by the PC + DAQ card to both PhS-OCT and HIFU every 4 ms)

3. Sample Preparation and Experimental setup

The sample used in this experimental setup is Agar 1% Phantom. The Agar powder (Fisher Scientific) was first mixed in hot water (approximately 90^{o}C) at 1:99 (Agar: water) weight-to-weight ratio. The mixture was then let to dissolve completely on hot plate with 100^{o}C temperature settings. The solution was then poured into a mold, which has the HIFU transducer fixed in place at the bottom of the mould.

The experimental setup is summarised as in Figure 4. A PC (Intel I7 4820K CPU, 16 GB DDR3 RAM). NI PCIe-6713 DAQ card (National Instruments Inc.) sends TTL trigger output and synchronises both the OCT and HIFU apparatus. The DAQ card then waits and collects data from the high-speed line-scan camera (SUI-LDH2, Sensors Ltd.), upon receiving internal trigger from the camera. There are 16 sets of experiments; each was repeated three times, dividing into two qualitative studies. The first study is to investigate the effect of increasing/reducing input voltage to the HIFU transducer; and the second study is to investigate the effect of increasing/reducing the number of cycles per pulse applied to HIFU transducer at fixed acoustic power output. The fixed acoustic power output was chosen so that when the minimum number of cycles in one HIFU pulse was selected, PhS-OCT could still give a good SNR (0.98 W acoustic output in this case).

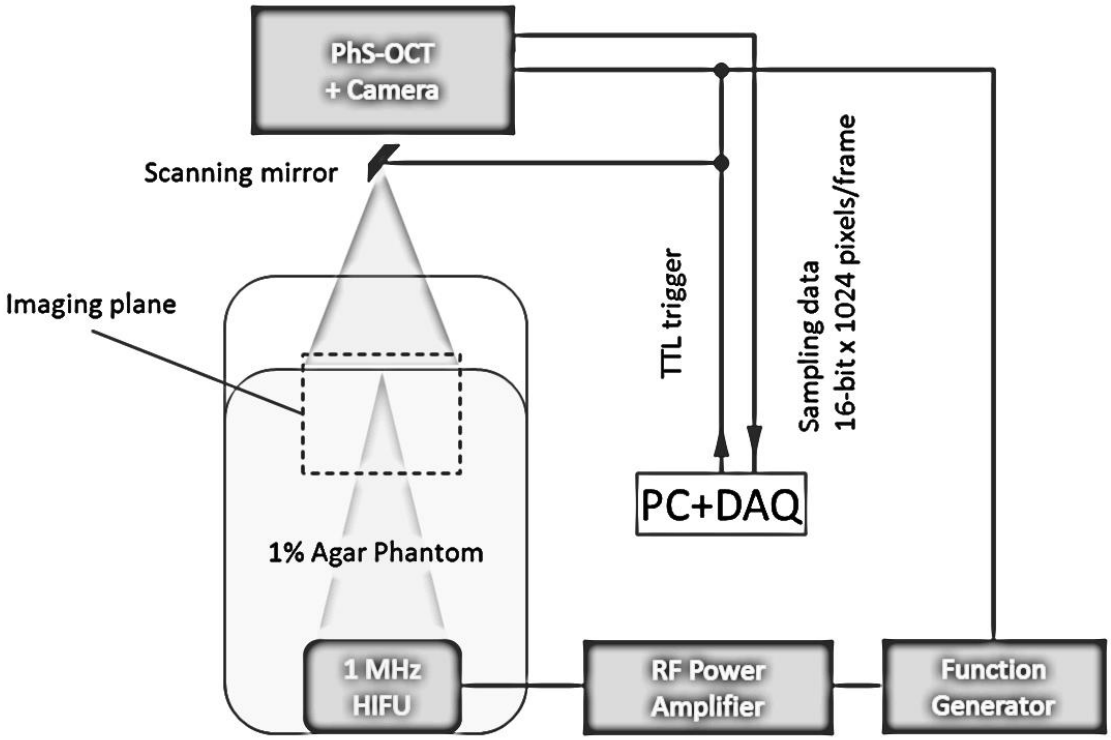

Figure 4: Schematic of experimental setup for PhS-OCT and HIFU transducer in order to capture HIFU-induced shear-wave

RESULTS AND DISCUSSIONS

1. Effect of HIFU acoustic power on Shear-wave generation

Once the shear-wave source is located by real-time tracking software, several sets of data were captured at slightly different imaging plane (approximately ±0.2 mm displacement in direction perpendicular to imaging plane). This step finds and confirms the location of the HIFU focus. The imaging plane that captured shear-wave source (HIFU focus) would yield strongest shear-wave displacement. The HIFU transducer (1.02 MHz) was set to output 100 cycles per pulse at 2.37 W acoustic power output for this confirmation step. The first capture was at 21.7 µs after the first HIFU pulse. The first obvious and observable displacement induced by the HIFU pulse is at 65 µs after the first TTL trigger. An example of the final confirmation step, which shows the time-evolution of shear-wave at the HIFU focus, is shown

in Figure 5. Once the position giving strongest shear-wave displacement is located, the sample was fixed for further experiments.

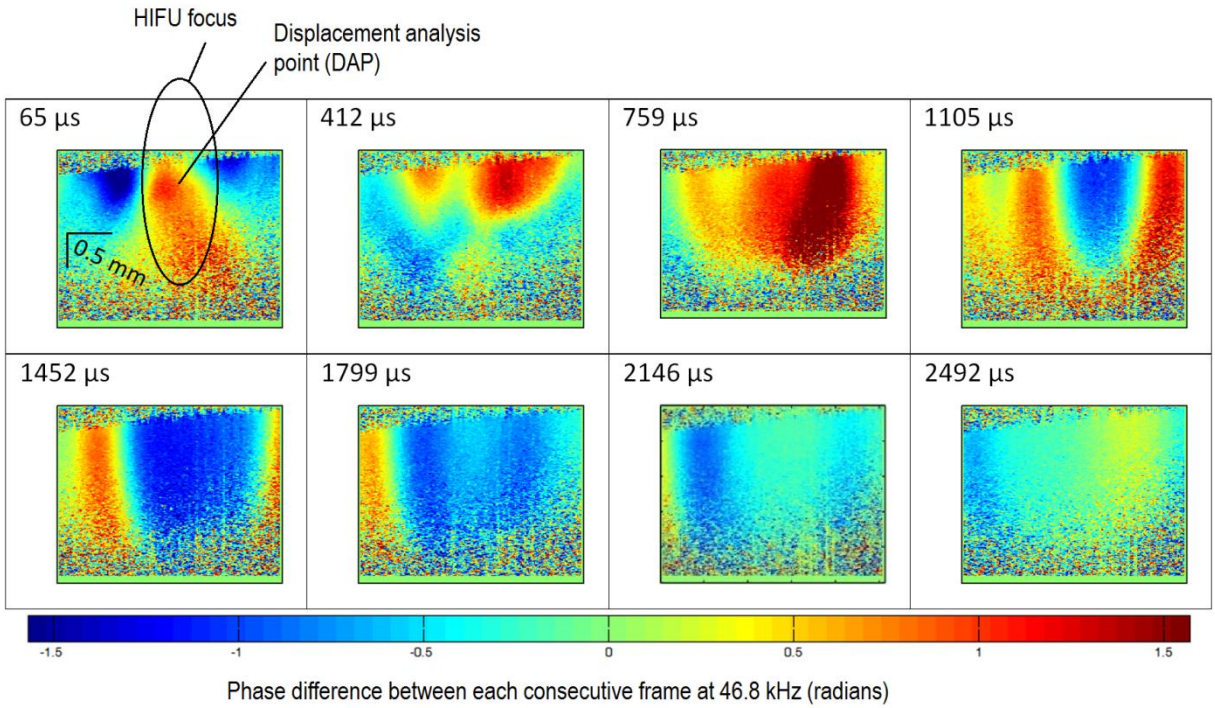

Figure 5: 2D map of phase differences between each consecutive frame at 46.8 kHz with respect to the time after the first TTL trigger, at the shear-wave source (HIFU focus, 1.02 MHz, 100 cycles/pulse at 2.37 W acoustic powers). The equivalent limit on scale bar is -117 nm to +117nm displacement difference between each consecutive frame at 46.8 kHz.

a)

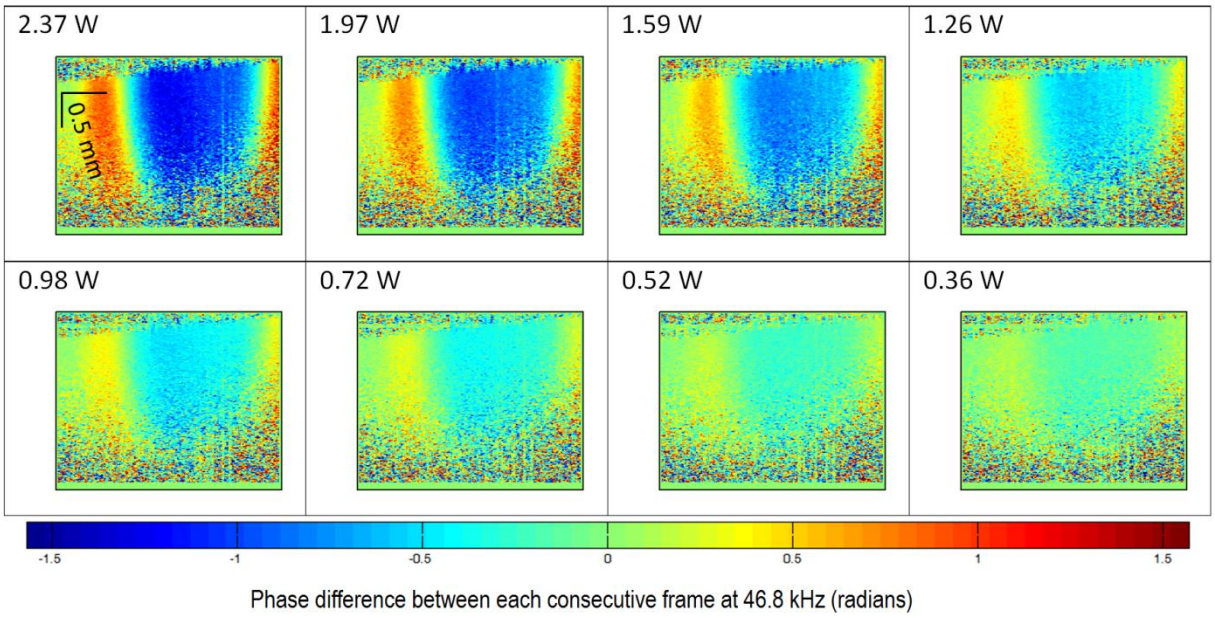

b)

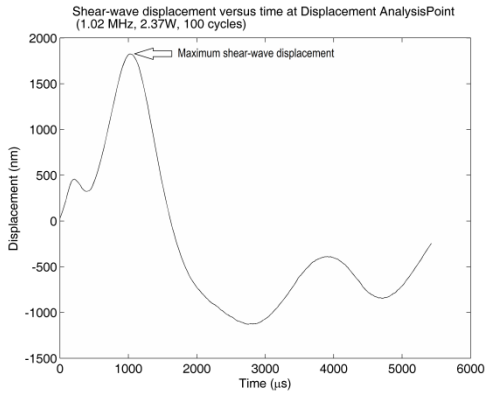

c)

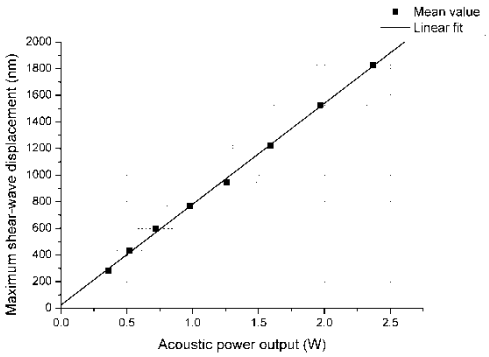

Figure 6 a) 2D map of phase difference (radians) with respect to different acoustic power output (W) at 1452 µs after first TTL trigger; b)Shear-wave displacement versus time at Displacement Analysis Point (DAP); c) Linear relationship between HIFU Acoustic power output and shear-wave displacement at DAP. The equivalent limit on scale bar is -117 nm to +117 nm displacement difference between each consecutive frame at 46.8 kHz.

The dataset for quantitative analysis are the phase differences $\Delta\phi$ between successive frames of A-scans, which are vertical lines (256 vertical lines in each frame). There are 256 frames in total, resulting in 255 frames of 2D (256 x A-scans) phase difference. The datasets of 2D phase difference are visualised with limits between –π/2 and + π/2, and can be easily converted to vertical displacement Δz by:

$$\Delta z(i,j,t) = \frac{\Delta\phi(i,j,t).\lambda}{4\pi n}$$

where i, j are the horizontal and vertical coordinates of a given pixel in the M-scan, t is the time difference between each A-scan, λ = 1310 nm is the superluminescent diode (OCT light source) central wavelength, and n is the sample refractive index (assumed to be 1.4 for this experiment).

The best frame for qualitative analysis of this study (HIFU power versus shear-wave displacement) is at 1452 µs (64 frames*21.67 µs) after the HIFU trigger signal. Eight different sets of PhS-OCT capture in different acoustic power and constant number of cycles per pulse (100 cycles per pulse at 1.02 MHz) are displayed on the same scale of phase difference (Figure 6a) for visual comparison.

The difference in shear-wave displacement versus different acoustic power settings can be quantified using displacement analysis point (refer to Figure 5). An example of the shear-wave displacement at the displacement analysis point (2.37 W, 1.02 MHz, 100 cycles/pulse) with respect to time is shown in Figure 6b. There is an unexpected negative bulk displacement after the first strong positive (+ve) push as indicated in Figure 6b. Further study into this bulk displacement could help understand more about the interaction of HIFU on this agar sample, and possibly on animal tissues.

Another interesting result from comparing the maximum (+ve) shear-wave displacement (refer to Figure 6b) versus the acoustic power output can be seen in Figure 6c. The maximum displacement for each acoustic power output was obtained from the displacement analysis point (DAP). A simple linear fitting model is proposed for the relationship between maximum shear-wave displacement and HIFU acoustic power output (1.02 MHz, 100 cycles/pulse):

$$max(\Delta z(DAP)) = a.P_{ac} + b$$

where $max(\Delta z(DAP))$ is the maximum shear-wave displacement at DAP, P_{ac} is the HIFU acoustic power output, a and b are linear fitting's parameters ($a = 758 \pm 11$ nm.W^{-1}, $b = 25 \pm 15$ nm). This model shows a very good linear relationship between the shear-wave displacement and the HIFU acoustic power output (Pearson's r = 0.9994). The maximum shear-wave displacement is approximately zero when the acoustic power output is at zero as predicted. Note that the error from HIFU acoustic power output measurement far exceeds the error from shear-wave displacement measurement.

This linear relationship provides a simple correlation between displacement field inside the with respect to the HIFU acoustic power output. Other imaging modalities with a fixed sensitivity to displacement detection would greatly benefit from this finding. Changing acoustic power output, above which HIFU-induced shear-wave is detectable for a given imaging system (with fixed spatial resolution), is one example.

2. Effect of number of cycles per pulse (HIFU) on Shear-wave generation

Although reducing the number of cycles per HIFU pulse is equivalent to reducing the total power deposited into the sample, the former is not exactly the same as the latter regarding HIFU-induced shear-wave. The objective of this study is to find whether there is a simple relationship between increasing/reducing the number of cycles per pulse with a fixed HIFU acoustic power output, and the HIFU-induced shear-wave displacement.

Similar to the first study, confirmation step was performed to determine the best time and location for the qualitative analysis. The evolution of HIFU-induced shear-wave over time was captured with the focus located at a) the same position as in previous study, as well as b) at the edge of the frame in this second experiment. The reason for the second imaging location is that: a) the shear-wave propagation

can be approximated as symmetric in homogenous sample (which can be seen in the previous study, Figure 5), b) there are more observations from HIFU-induced shear-wave that occurs relatively far away from the focus, and c) minimising the range of imaging reduces data acquisition and processing time.

The observation from the second imaging location shows that more fringes are produced almost at the same instance (Figure 7) after the first trigger. This phenomenon suggests a more complex interaction between HIFU pulse and the agar sample. We attribute this observation to the side lobes of the HIFU pressure field. However, more work is required to confirm that the spacing of the side lobes is similar to the spacing of shear-wave from the very first set of result.

Qualitative analysis of the PhS-OCT data in this position also delivers better propagation characteristics of the HIFU-induced shear-wave, e.g. shear-wave speed and shear-wave dispersion.

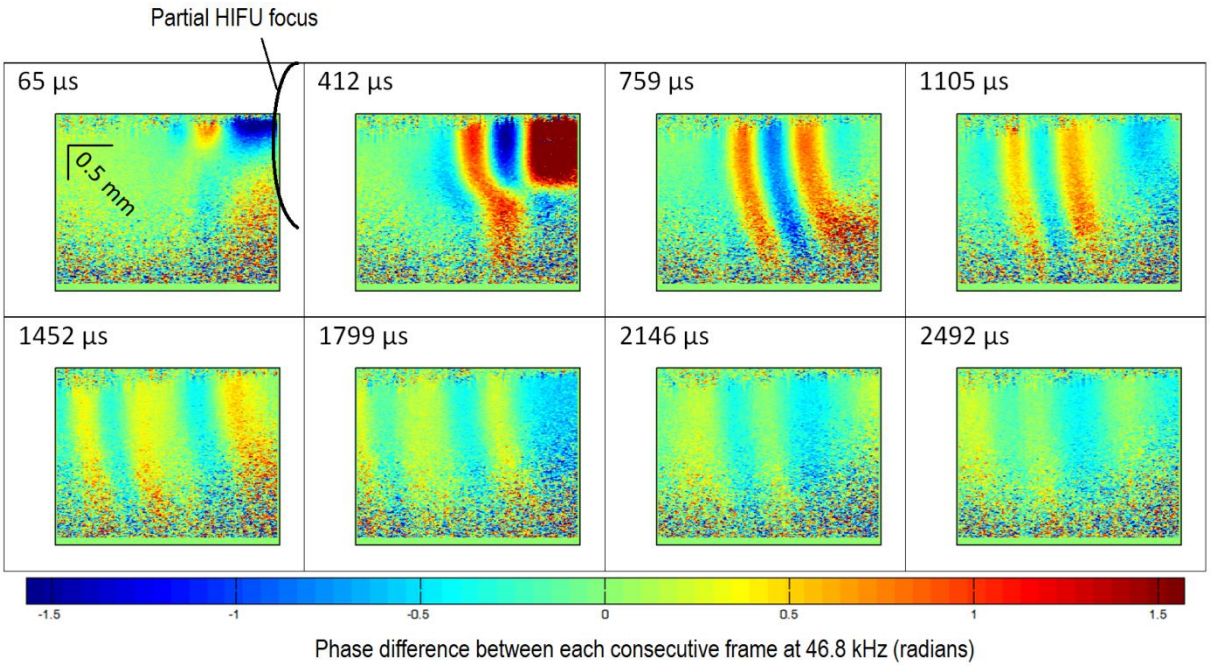

Figure 7: 2D map of phase differences between each consecutive frame (46.8 kHz) at different time, with respect to the TTL trigger time; HIFU operates at 2.37 W acoustic power output, 100 cycles/pulse. The equivalent limit on scale bar is -117 nm to +117 nm **displacement difference between each consecutive frame at 46.8 kHz.**

a)

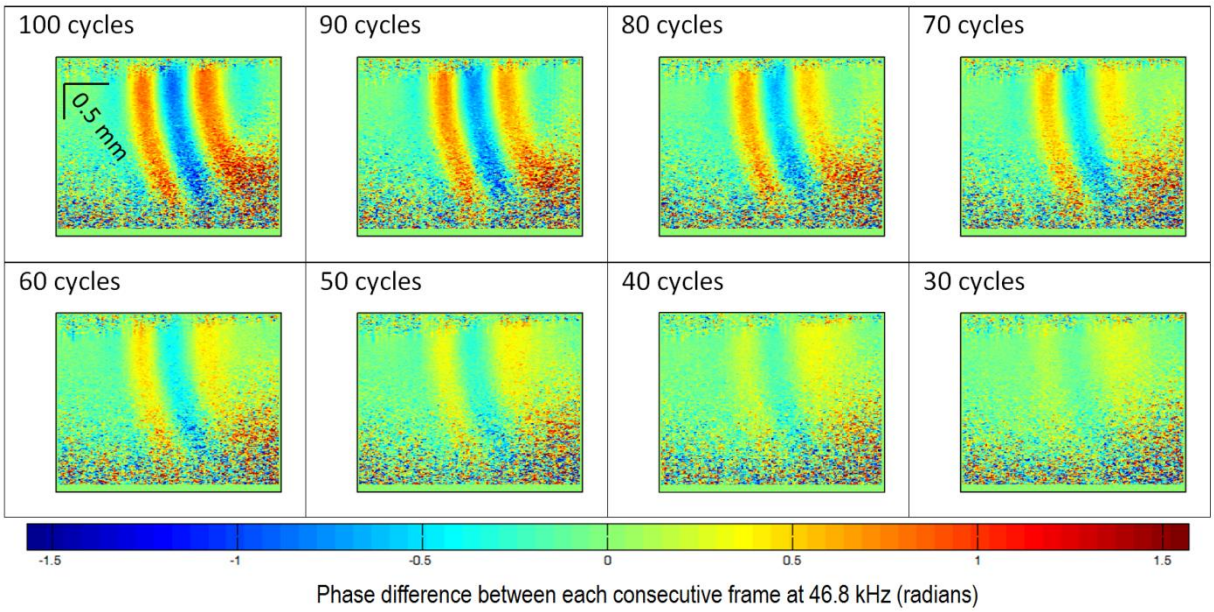

b)

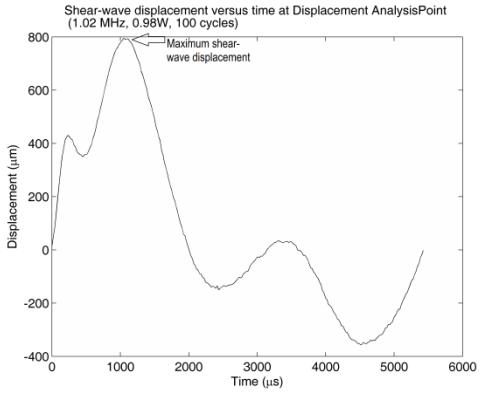

c)

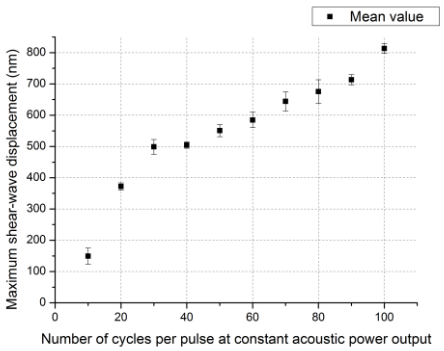

Figure 8 a) HIFU-induced shear-wave with reducing number of cycles per pulse at 759 μs after HIFU is triggered (2.37 W acoustic power, 100 cycles/pulse); b) Shear-wave displacement versus time at Displacement Analysis Point (DAP) with HIFU operating at 0.98 W acoustic power, 100 cycles/pulse; c) plot of number of cycles per pulse versus shear-wave displacement at DAP (constant 0.98 W acoustic power). The equivalent limit on scale bar is -117 nm to +117 nm displacement difference between each consecutive frame at 46.8 kHz.

As described in the first study for quantitative analysis, an example of the shear-wave displacement (HIFU 1.02 MHz, 2.37 W, 100 cycles/pulse) versus time at DAP (referred to Figure 5 for DAP) is shown in Figure 8b. The imaging location and the position of HIFU focus remain the same as in previous study. This imaging location should not be confused with the imaging location which is shown in Figure 7 and 8a (discussed in previous paragraph).

Assuming the acoustic power output per pulse cycle is constant, the error in measurement (of the relationship between number of cycles per pulse versus the shear-wave displacement) is dominated by the error in measuring the shear-wave displacement. The mean and error were therefore calculated from repeated data acquisition (3 samples per set) in each dataset of different cycle per pulse versus shear-wave displacement. Figure 8c shows the relationship to be adequately linear from 30 to 100 cycles/pulse, but less so at lower number of cycles per pulse (<40 cycles/pulse). Since the shear-wave displacement should drop to zero when the number of cycle per HIFU pulse becomes zero, a sharp drop appears to start from the 30 cycles per pulse. This non-linear relationship at 30 cycles/pulse is possibly attributed by the non-linear characteristic of the HIFU transducer. The transducer may require high (enough) number of cycles per pulse to reach constant acoustic power output.

3. Further work on PhS-OCT setup for HIFU, and current limitations

PhS-OCT could quantitatively analyse the interaction of HIFU in agar sample at sub-therapeutic power level. Further work will explore into the interaction of HIFU in biological tissues using PhS-OCT in order to confirm the usefulness of this system in clinical applications.

Apart from the HIFU acoustic power output and number of cycles per pulse, other acoustic parameters such as frequency and F-number could also be significant regarding HIFU-induced shear-wave. The effects of said parameters on HIFU-induced shear-wave within biological tissues are not very well-understood until now. Effect of different acoustic parameters on the induction of shear-wave can be quantitatively analysed. Once the findings are large and reliable enough, shear-wave displacement

could be mapped accurately with respect to any HIFU transducer's parameters. Many imaging techniques would benefit from these quantitative results. E.g. for ultrasound-guided HIFU with a fixed imaging (axial) resolution, HIFU transducer can be designed to induce shear-wave with displacement well above the imaging resolution. Further investigations on this subject would greatly improve the design of HIFU transducer for planning and tracking efforts.

Although superior in terms of spatial and temporal resolution, PhS-OCT suffers from limited penetration depth, typically operating within only a few millimetres from the sample's surface. This limitation exacerbates the measurement where the acoustic impedance mismatch between air and sample is relatively large. Our initial observations reveal that the acoustic impedance mismatch might have enhanced HIFU-induced shear-wave phenomenon. Therefore, the sample may need a coupling material that is both optically transparent under PhS-OCT, and acoustically similar to the sample's acoustic impedance.

The HIFU transducer in this experiment operates at maximum 2.37 W (spatial-average pulse-average intensity $\mathrm{I}_{SAPA} = 97\ \mathrm{W.\,cm^{-2}}$ at maximum acoustic power). Since the objective of this paper is to detect and track HIFU focus with minimum damage to sample (reducing total acoustic power), the acoustic power output from the HIFU is far less than the therapeutic HIFU transducer's acoustic output, which is typically a few hundreds of $\mathrm{W.cm^{-2}}$ (9).

CONCLUSIONS

PhS-OCT displays exceptional capabilities in tracking, detecting and calibrating High-Intensity Focused Ultrasound (HIFU) focus. The system can detect HIFU-induced shear-wave with HIFU acoustic power output set to as low as 0.36 W (or spatial-average pulse-average intensity $\mathrm{I}_{SAPA} = 11\ \mathrm{W.\,cm^{-2}}$, 100 cycles/pulse at 1.02 MHz). High spatial and temporal resolution from PhS-OCT means that it can

be used to calibrate any HIFU device, correlating the displacement of HIFU-induced shear-wave with different HIFU power settings, and/or different physical characteristics of HIFU.

Further study in PhS-OCT guided HIFU can also employ needle OCT to track and detect HIFU focus within deep tissue region. This is the minimal invasive procedure where needle OCT is inserted into the region of interest for imaging, and could be used to guide HIFU treatment upon the development of this technique.

The most important aspect of this work is to demonstrate the potential of studying HIFU interaction with tissue sample in-depth, or specifically HIFU-induced shear-wave. Predictions of tissue behaviour under certain HIFU power settings would drastically improve. Therefore, further findings on this subject would benefits other imaging modalities to employ better HIFU power settings for appropriate tracking and detection.

There are a few limitations in building up and operating PhS-OCT for HIFU guidance. The cost of the system is one, and is approximated to be between an ultrasound and MRI systems. The cost multiplies for building and maintaining such system. However, the biggest disadvantage in PhS-OCT is the low penetration depth and therefore limits the number of PhS-OCT's clinical applications.

A more standardised PhS-OCT imaging protocol is required to characterise the shear-wave more consistently, i.e. choosing the best time after the first HIFU trigger, and the best location for imaging.

TABLES AND FIGURES

Figure 1: a) Relative intensity map and b) logarithm intensity map of the HIFU transducer in the axial plane of the focus 6
Figure 2 Signal generator's input signal vs. HIFU acoustic power output 7
Figure 3: Scanning protocols for PhS-OCT and HIFU transducer for 2D capture of HIFU-induced shear-wave. (TTL trigger is sent by the PC + DAQ card to both PhS-OCT and HIFU every 4 ms) 9
Figure 4: Schematic of experimental setup for PhS-OCT and HIFU transducer in order to capture HIFU-induced shear-wave 10
Figure 5: 2D map of phase differences between each consecutive frame at 46.8 kHz with respect to the time after the first TTL trigger, at the shear-wave source (HIFU focus, 1.02 MHz, 100 cycles/pulse at 2.37 W acoustic powers). The equivalent limit on scale bar is -117 nm to +117nm displacement difference between each consecutive frame at 46.8 kHz. 12
Figure 6 a) 2D map of phase difference (radians) with respect to different acoustic power output (W) at 1452 µs after first TTL trigger; b)Shear-wave displacement versus time at Displacement Analysis Point (DAP); c) Linear relationship between HIFU Acoustic power output and shear-wave displacement at DAP. The equivalent limit on scale bar is -117 nm to +117 nm displacement difference between each consecutive frame at 46.8 kHz. 13
Figure 7: 2D map of phase differences between each consecutive frame (46.8 kHz) at different time, with respect to the TTL trigger time; HIFU operates at 2.37 W acoustic power output, 100 cycles/pulse. The equivalent limit on scale bar is -117 nm to +117 nm displacement difference between each consecutive frame at 46.8 kHz. 17
Figure 8 a) HIFU-induced shear-wave with reducing number of cycles per pulse at 759 µs after HIFU is triggered (2.37 W acoustic power, 100 cycles/pulse); b) Shear-wave displacement versus time at Displacement Analysis Point (DAP) with HIFU operating at 0.98 W acoustic power, 100 cycles/pulse; c) plot of number of cycles per pulse versus shear-wave displacement at DAP (constant 0.98 W acoustic power). The equivalent limit on scale bar is -117 nm to +117 nm displacement difference between each consecutive frame at 46.8 kHz. 18

REFERENCE

1. Ter Haar GR. High Intensity Focused Ultrasound for the Treatment of Tumors. Echocardiography. 2001;18(4):317-22.
2. Bihan DL, Delannoy J, Levin RL. Temperature mapping with MR imaging of molecular diffusion: application to hyperthermia. Radiology. 1989;171(3):853-7. PubMed PMID: 2717764.
3. Bohris C, Schreiber WG, Jenne Ju, Simiantonakis I, Rastert R, Zabel HJ, et al. Quantitative MR temperature monitoring of high-intensity focused ultrasound therapy. Magnetic Resonance Imaging. 1999 5//;17(4):603-10.
4. Tempany CMC, Stewart EA, McDannold N, Quade BJ, Jolesz FA, Hynynen K. MR Imaging–guided Focused Ultrasound Surgery of Uterine Leiomyomas: A Feasibility Study. Radiology. 2003;226(3):897-905. PubMed PMID: 12616023.
5. Vaezy S, Shi X, Martin RW, Chi E, Nelson PI, Bailey MR, et al. Real-time visualization of high-intensity focused ultrasound treatment using ultrasound imaging. Ultrasound in Medicine & Biology. 2001;27(1):33-42.
6. Bercoff J, Pernot M, Tanter M, Fink M. Monitoring thermally-induced lesions with supersonic shear imaging. Ultrasonic Imaging. 2004;26(2):71-84.
7. Song S, Huang Z, Nguyen T-M, Wong EY, Arnal B, O'Donnell M, et al. Shear modulus imaging by direct visualization of propagating shear waves with phase-sensitive optical coherence tomography. Journal of Biomedical Optics. 2013;18(12):121509-.
8. Bercoff J, Tanter M, Fink M. Supersonic shear imaging: a new technique for soft tissue elasticity mapping. Ultrasonics, Ferroelectrics, and Frequency Control, IEEE Transactions on. 2004;51(4):396-409.
9. Ebbini ES, Ter Haar G. Ultrasound-guided therapeutic focused ultrasound: Current status and future directions. International Journal of Hyperthermia. 2015 2015/02/17;31(2):77-89.